

Theory of Magnetic Properties and Spin-Wave Dispersion for Ferromagnetic (Ga,Mn)As

Jürgen König,^{1,2} Tomas Jungwirth,^{1,2,3} and A. H. MacDonald^{1,2}

¹*Department of Physics, University of Texas, Austin, TX 78712, USA*

²*Department of Physics, Indiana University, Bloomington, IN 47405, USA*

³*Institute of Physics ASCR, Cukrovarnická 10, 162 00 Praha 6, Czech Republic*

(December 2, 2024)

We present a microscopic theory of the long-wavelength magnetic properties of the ferromagnetic diluted magnetic semiconductor (Ga,Mn)As. Details of the host semiconductor band structure, described by a six-band Kohn-Luttinger Hamiltonian, are taken into account. We relate our quantum-mechanical calculation to the classical micromagnetic energy functional and determine anisotropy energies and exchange constants. We find that the exchange constant is substantially enhanced compared to the case of a parabolic heavy-hole-band model.

PACS numbers: 75.50.Pp, 75.30.Ds, 75.30.Gw

I. INTRODUCTION

The recent discovery of carrier-mediated ferromagnetism in diluted magnetic semiconductors (DMS) has generated intense interest, in part because it suggests the prospect of developing devices which combine information processing and storage functionalities in one material.^{1–19} Ferromagnetism has been observed in Mn doped GaAs up to critical temperatures T_c of 110K (see Ref. 9). Doping a III-V compound semiconductor with Mn introduces both local magnetic moments, with concentration N_{Mn} and spin $S = 5/2$, and itinerant valence-band carriers with density p and spin $s = 1/2$. An antiferromagnetic interaction between both kinds of spin mediates an effective ferromagnetic interaction between Mn²⁺ spins.

A phenomenological long-wavelength description of ferromagnets usually requires only a small set of characteristic parameters. For example, a ferromagnet which possesses an uniaxial anisotropy can be modeled by a classical micromagnetic energy functional $E[\hat{\mathbf{n}}(\mathbf{r})]$,

$$E[\hat{\mathbf{n}}(\mathbf{r})] = E_0 + \int d^3r \left[K \sin^2 \theta + A (\nabla \hat{\mathbf{n}})^2 \right], \quad (1)$$

where $\hat{\mathbf{n}}(\mathbf{r})$ is the unit vector that specifies the (space-dependent) local Mn spin orientation, and θ is its angle with respect to the easy axis. The dependence on the orientation of the magnetic moment is parametrized by the anisotropy constant K . The exchange constant (or spin stiffness) A governs the energy cost to twist the orientations of adjacent spins relative to each other. Together with the saturation moment $\mu_0 M_s$ and the magnetostatic energy, dropped for convenience in Eq. (1), the parameters K and A determine a whole variety of magnetic properties such as²⁰ domain-wall width δ_B , domain-wall energy per area γ , exchange length l_{ex} , hardness parameter κ , single-domain radius R_{sd} , and anisotropy field $\mu_0 H_0$. In addition they determine the energy cost Ω_k of

collective long-wavelength spin excitations, spin waves. For uniaxial anisotropy the quantized energy is

$$\Omega_k = \frac{2K}{M_s/(g\mu_B)} + \frac{2A}{M_s/(g\mu_B)} k^2, \quad (2)$$

at wavevector k . Here, g is the g -factor and μ_B the Bohr magneton. The spin-wave dispersion has an energy gap which is determined by the anisotropy K . The spin exchange constant A defines the curvature of the spin-wave dispersion.

The purpose of the present paper is to present a microscopic theory for the phenomenological parameters which characterize (Ga,Mn)As as a ferromagnet. The form of the micromagnetic energy functional appropriate to the symmetry of the crystal will be addressed in Sec. IV. We expect that these predictions will be useful in interpreting experimental studies of these semiconductor's magnetic properties. The search for the carrier density, Mn concentration and (III,Mn)V compound semiconductor material for which the critical temperature has its maximum value is, perhaps, the most important endeavor in this research area. It has been guided to date by mean-field-theory^{21–26} considerations that neglect the low-energy correlated magnetization fluctuations characterized by M_s , K , and A . However, as we have emphasized earlier,^{27–30} small exchange can also limit the temperature at which long-range magnetic order can be maintained.

In recent work^{27–29} we developed a theory of diluted magnetic semiconductor ferromagnetism which accounts for dynamic correlations in the ordered state. For simplicity we used parabolic bands for the itinerant carriers, leading to isotropic ferromagnetism. We found, in addition to the usual spin-wave mode (which was, due to Goldstone's theorem, gapless for this simple model), a continuum of Stoner excitations, and another collective branch of excitations, optical spin waves. As we have shown,^{27,30} the low-energy Goldstone modes can suppress the critical temperature in comparison to mean-field es-

timates and can even change trends in T_c as a function of the system's parameters.

To address anisotropy one has to go beyond a parabolic-band model and take details of the band structure into account. The itinerant-carrier bands are p -type and reflect the crystal symmetry of the underlying lattice. Due to spin-orbit coupling the spin degrees of freedom also feel the crystal anisotropy. We will use a six-band description based on the Kohn-Luttinger Hamiltonian to model the (Ga,Mn)As valence bands. Mean-field calculations^{23,25,26} as well as Monte Carlo studies³¹ based on this more realistic band structure have been performed recently to address magnetic anisotropy effects and explore trends in the critical temperature.

In Sec. II we set the starting point of our theory by deriving a formal expression for the effective action for the Mn impurity spins after integration out the itinerant carriers. This formal development generalizes earlier work^{27–29} to general spin-orbit coupled band models. Using the effective action we numerically determine the zero-temperature spin-wave dispersion in Sec. III. Then, in Sec. IV we establish the connection between our spin-wave results and the classical micromagnetic energy functional, adjusted to the symmetry defined by the crystal structure. Finally, in Sec. V, we present numerical results for the spin-wave dispersion and the exchange constant. We find that for parameter range of interest the exchange constant is enhanced by up to an order of magnitude compared to naive results obtained earlier, in which light-hole bands were neglected and the heavy-hole bands were approximated as parabolic.

II. HAMILTONIAN AND EFFECTIVE ACTION

Our theory is based on the following model. Magnetic ions with spin $S = 5/2$ at positions \mathbf{R}_I are antiferromagnetically coupled to valence-band carriers described by an envelope-function approach,

$$H = H_0 + J_{pd} \int d^3r \mathbf{S}(\mathbf{r}) \cdot \mathbf{s}(\mathbf{r}), \quad (3)$$

where $\mathbf{S}(\mathbf{r}) = \sum_I \mathbf{S}_I \delta(\mathbf{r} - \mathbf{R}_I)$ is the impurity-spin density and $J_{pd} > 0$. We approximate the impurity-spin density by a continuous functions (instead of a sum of delta functions). Provided that J_{pd} is not strong enough to localize valence-band carriers near the Mn sites and the average distance between two Mn ions is small in comparison to the Fermi wavelength of the itinerant carriers, this approximation can be justified. The itinerant-carrier spin density is expressed in terms of carrier field operators by $\mathbf{s}(\mathbf{r}) = \sum_{ij} \Psi_i^\dagger(\mathbf{r}) \mathbf{s}_{ij} \Psi_j(\mathbf{r})$ where i and j label the basis in Hilbert space of spin and orbital angular momentum, and \mathbf{s}_{ij} is the corresponding representation of the spin operator. The envelope-function Hamiltonian H_0 for the valence bands can be parametrized by a small number

of symmetry-adapted parameters, the Luttinger parameters γ_1 , γ_2 , γ_3 , and the spin-orbit coupling Δ_{so} which splits the six states at the band edge into a quartet and a doublet. For explicit expressions of H_0 as well as representations of the spin matrices in a coordinate system in which the x , y , and z -axis are along the crystal axes, we refer to Eqs. (A8)-(A10) of Ref. 25, based on the Kohn-Luttinger Hamiltonian.³²

We note that local-spin-density-approximation electronic structure calculations,³³ taken at face value, find a strong hybridization between p and d carriers, which is not completely consistent with the model we use. However, given the overwhelming success^{3,4} of the present model in the case of paramagnetic (II,Mn)VI materials, we find it unlikely that the Mn d electrons are itinerant. If they were, the phenomenological approach we study here would be incomplete.

Our treatment of the Mn spin system as a continuum greatly simplifies our calculation by eliminating disorder associated with randomness in the Mn spin configuration. We do anticipate that the disorder can influence both anisotropy and exchange constant at the low- and high-carrier-concentration extremes. These effects are, however, outside the scope of the present study. We will identify several important features of the microscopic physics in the disorder-free model that we expect to be robust.

Our first goal is to integrate out the itinerant carriers and arrive at an effective description for the impurity-spin degrees of freedom. We use the Holstein-Primakoff (HP) representation³⁴ for the impurity spins. For small fluctuations around its mean-field polarization, we can approximate the spin operators by

$$S^+(\mathbf{r}) \approx b(\mathbf{r}) \sqrt{2N_{Mn}S} \quad (4)$$

$$S^-(\mathbf{r}) \approx b^\dagger(\mathbf{r}) \sqrt{2N_{Mn}S} \quad (5)$$

$$S^z(\mathbf{r}) = N_{Mn}S - b^\dagger(\mathbf{r})b(\mathbf{r}) \quad (6)$$

with bosonic fields $b^\dagger(\mathbf{r}), b(\mathbf{r})$. The quantization axis z is chosen here along the zero-temperature spin orientation (which might or might not coincide with a crystal axis, see Sec. IV). The partition function can be expressed as a coherent-state path integral in imaginary times:

$$Z = \int \mathcal{D}[\bar{z}z] \mathcal{D}[\bar{\Psi}\Psi] e^{-\int_0^\beta d\tau L(\bar{z}z, \bar{\Psi}\Psi)} \quad (7)$$

with $L = \int d^3r [\bar{z}\partial_\tau z + \sum_i \bar{\Psi}_i \partial_\tau \Psi_i] + H(\bar{z}z, \bar{\Psi}\Psi)$. The bosonic (impurity spin) and fermionic (itinerant carrier) degrees of freedom are labeled by the complex variables \bar{z}, z and the Grassmann numbers $\bar{\Psi}_i, \Psi_i$, respectively.

Since the Hamiltonian is bilinear in fermionic fields, we can integrate out the itinerant carriers and arrive at an effective description in terms of the localized spin density only, $Z = \int \mathcal{D}[\bar{z}z] \exp(-S_{\text{eff}}[\bar{z}z])$ with the action

$$S_{\text{eff}}[\bar{z}z] = S_{\text{BP}}[\bar{z}z] - \ln \det [(G^{\text{MF}})^{-1} + \delta G^{-1}(\bar{z}z)] , \quad (8)$$

where $S_{\text{BP}}[\bar{z}z] = \int_0^\beta d\tau \int d^3r \bar{z}\partial_\tau z$ is the usual Berry's phase term. In Eq. (8), we have already split the total kernel G^{-1} into a mean-field part $(G^{\text{MF}})^{-1}$ and a fluctuating part δG^{-1} ,

$$(G^{\text{MF}})_{ij}^{-1} = (\partial_\tau - \mu) \delta_{ij} + \langle i|H_0|j\rangle + N_{\text{Mn}} J_{\text{pd}} S s_{ij}^z \quad (9)$$

$$\delta G_{ij}^{-1}(\bar{z}z) = \frac{J_{\text{pd}}}{2} \left[(zs_{ij}^- + \bar{z}s_{ij}^+) \sqrt{2N_{\text{Mn}}S} - 2\bar{z}zs_{ij}^z \right] \quad (10)$$

where μ denotes the chemical potential, and i and j range over a complete set of hole-band states. In the following we define $\Delta = N_{\text{Mn}} J_{\text{pd}} S$ which is the mean-field energy to flip the spin of an itinerant carrier. The physics of the itinerant carriers is embedded in the effective action of the magnetic ions. It is responsible for the retarded and non-local character of the interactions between magnetic ions.

III. INDEPENDENT SPIN-WAVE THEORY

Independent spin-wave theory is obtained by expanding Eq. (8) up to quadratic order in z and performing Matsubara imaginary time and space Fourier transforms. Since δG^{-1} is at least linear in z we can truncate the series

$$S_{\text{eff}}[\bar{z}z] = \sum_{n=0}^{\infty} S_{\text{eff}}^{(n)}[\bar{z}z], \quad (11)$$

after $n = 2$, where n denotes the order in δG^{-1} . The zeroth-order contribution, $S_{\text{eff}}^{(0)}[\bar{z}z] = S_{\text{BP}}[\bar{z}z] - \ln \det(G^{\text{MF}})^{-1}$ contains the Berry's phase term

$$S_{\text{BP}}[\bar{z}z] = \sum_{m,\mathbf{k}} (-i\nu_m) \bar{z}(\mathbf{k}, \nu_m) z(\mathbf{k}, \nu_m), \quad (12)$$

and the mean-field contribution from the itinerant carriers, which is independent of the bosonic fields z and \bar{z} . Here, ν_m are the bosonic Matsubara frequencies.

The next term of the expansion, $S^{(1)}[\bar{z}z] = -\text{tr}(G^{\text{MF}} \delta G^{-1})$, reads in Fourier representation

$$\begin{aligned} S_{\text{eff}}^{(1)}[\bar{z}z] &= \frac{J_{\text{pd}}}{(\beta V)^2} \sum_{n,\mathbf{q}} \sum_{ij} G_{ij}^{\text{MF}}(\mathbf{q}, \omega_n) s_{ji}^z \\ &\quad \times \sum_{m,\mathbf{k}} \bar{z}(\mathbf{k}, \nu_m) z(\mathbf{k}, \nu_m), \end{aligned} \quad (13)$$

plus terms linear in z and \bar{z} . Here, ω_n and ν_m are fermionic and bosonic Matsubara frequencies, respectively. To determine the mean-field Green's functions we diagonalize the matrix $\langle i|H_0(\mathbf{q}) + \Delta s^z|j\rangle$ for each wavevector \mathbf{q} and denote eigenvalues and eigenstates by $\epsilon_\alpha(\mathbf{q})$ and $|\alpha\rangle$, respectively. Since the itinerant-carrier spin density $\langle \mathbf{s} \rangle = (1/V) \sum_{\mathbf{q}} \sum_\alpha f[\epsilon_\alpha(\mathbf{q})] \langle \alpha | \mathbf{s} | \alpha \rangle$ is aligned antiparallel to the impurity spin-polarization axis (otherwise this would not be an easy axis), the terms linear in z and \bar{z} drop out, and we get

$$S_{\text{eff}}^{(1)}[\bar{z}z] = \frac{J_{\text{pd}} p \xi}{2\beta V} \sum_{m,\mathbf{k}} \bar{z}(\mathbf{k}, \nu_m) z(\mathbf{k}, \nu_m), \quad (14)$$

where $\xi = -2\langle s^z \rangle / p$ is the fractional itinerant-carrier polarization, $0 \leq \xi \leq 1$.

For the second-order term of the expansion, $S_{\text{eff}}^{(2)}[\bar{z}z] = \frac{1}{2} \text{tr}(G^{\text{MF}} \delta G^{-1} G^{\text{MF}} \delta G^{-1})$, we find in Fourier representation

$$\begin{aligned} S_{\text{eff}}^{(2)}[\bar{z}z] &= \frac{N_{\text{Mn}} J_{\text{pd}}^2 S}{4\beta V^2} \sum_{m,\mathbf{q},\mathbf{k}} \sum_{\alpha\beta} \frac{f[\epsilon_\alpha(\mathbf{q})] - f[\epsilon_\beta(\mathbf{q} + \mathbf{k})]}{i\nu_m + \epsilon_\alpha(\mathbf{q}) - \epsilon_\beta(\mathbf{q} + \mathbf{k})} \\ &\quad \left[2s_{\alpha\beta}^+ s_{\beta\alpha}^- \bar{z}(\mathbf{k}, \nu_m) z(\mathbf{k}, \nu_m) \right. \\ &\quad \left. + s_{\alpha\beta}^+ s_{\beta\alpha}^+ \bar{z}(\mathbf{k}, \nu_m) \bar{z}(-\mathbf{k}, -\nu_m) \right. \\ &\quad \left. + s_{\alpha\beta}^- s_{\beta\alpha}^- z(\mathbf{k}, \nu_m) z(-\mathbf{k}, -\nu_m) \right] + \mathcal{O}(z^3), \end{aligned} \quad (15)$$

with $s_{\alpha\beta}^\pm = \langle \alpha | s^\pm | \beta \rangle$ and $s_{\beta\alpha}^\pm = \langle \beta | s^\pm | \alpha \rangle$. Note, that the indices α and β label the single-particle eigenstates for valence-band carriers with *different* wavevectors, namely \mathbf{q} and $\mathbf{q} + \mathbf{k}$, respectively.

The Matsubara frequency ν_m in the denominator on the r.h.s of Eq. (15) accounts for the dynamics of the itinerant carriers. This frequency dependence is crucial to account for the existence of the Stoner spin-flip continuum and the optical spin-wave mode. On the other hand, the existence of the usual spin wave follows already from the static limit (i.e., when the frequency dependence in the denominator in Eq. (15) is dropped), and the spin-wave dispersion is described rather accurately.

The sum of Eqs. (12), (14), and (15) is a quadratic form in the bosonic fields z and \bar{z} . The zeros of the kernel define the spin-wave energies $\Omega_{\mathbf{k}}$ as a function of momentum \mathbf{k} (after analytic continuation $i\nu_m \rightarrow \Omega + i0^+$). In the following we go the static limit as discussed above. We define the quantities

$$E_{\mathbf{k}}^{\sigma\sigma'} = -\frac{1}{V} \sum_{\mathbf{q}} \sum_{\alpha\beta} \frac{f[\epsilon_\alpha(\mathbf{q})] - f[\epsilon_\beta(\mathbf{q} + \mathbf{k})]}{\epsilon_\alpha(\mathbf{q}) - \epsilon_\beta(\mathbf{q} + \mathbf{k})} s_{\alpha\beta}^\sigma s_{\beta\alpha}^{\sigma'} \quad (16)$$

with $\sigma, \sigma' = \pm$, and perform a Bogoliubov transformation, which finally yields

$$\frac{\Omega_{\mathbf{k}}}{\Delta} = \frac{J_{\text{pd}}}{2} \sqrt{\left(\frac{p\xi}{\Delta} - E_{\mathbf{k}}^{+-} \right)^2 - |E_{\mathbf{k}}^{++}|^2}. \quad (17)$$

From the definition Eq. (16) we see that $E_{\mathbf{k}}^{+-}$ is real and $E_{\mathbf{k}}^{--} = (E_{\mathbf{k}}^{++})^*$. Equation (17) is the central result of this section. The remaining task is to evaluate the fractional itinerant-carrier polarization ξ and the quantities $E_{\mathbf{k}}^{+-}$ and $E_{\mathbf{k}}^{++}$ numerically.

Before we carry on with establishing the relation between Eq. (17) and micromagnetic parameters of a classical energy functional, we make three remarks:

(i) Correlation effects among the Mn spins, which are not described by the mean-field picture, enter our theory

via the contribution $S_{\text{eff}}^{(2)}[\bar{z}z]$. To reduce our theory to the mean-field level we would have to neglect this term, i.e., truncate the series Eq. (11) already after $n = 1$. In this case, the energy $\Omega^{\text{MF}} = J_{\text{pd}}p\xi/2$ of a Mn spin excitation would be dispersionless and by a factor of $p\xi/(2N_{\text{Mn}}S)$ smaller than the mean-field energy Δ to flip an itinerant-carrier spin. Due to correlations between Mn and band-spin orientations, however, the spin-wave energy $\Omega_{\mathbf{k}}$ is always smaller than Ω^{MF} .

(ii) In the absence of spin-orbit coupling all products of the form $s_{\alpha\beta}^+s_{\beta\alpha}^+$ or $s_{\alpha\beta}^-s_{\beta\alpha}^-$ vanish. As a consequence, $E_{\mathbf{k}}^{++} = E_{\mathbf{k}}^{--} = 0$ for all \mathbf{k} . This statement is even true for finite spin-orbit coupling in case when the valence bands are isotropic.

(iii) To go beyond the static limit, we may expand the fraction on the r.h.s of Eq. (15) up to linear order in $i\nu_m$. As shown in Appendix A, this linear correction simply amounts to a renormalization of the Berry's phase term by replacing $\Omega \rightarrow \Omega(1 - x)$. In the absence of spin-orbit coupling we find that x is just the ratio of the spin densities, $x = \langle s^z \rangle / (N_{\text{Mn}}S)$, where $\langle \dots \rangle = (1/V) \sum_{\mathbf{q}} \sum_{\alpha} f[\epsilon_{\alpha}(\mathbf{q})] \langle \alpha | \dots | \alpha \rangle$. For finite spin-orbit coupling but with a band Hamiltonian that is invariant under rotation in space, the spin s^z has to be replaced by the total angular momentum $s^z + l^z$, i.e., we find $x = \langle s^z + l^z \rangle / (N_{\text{Mn}}S)$.

The renormalization factor $(1 - x)$ indicates that in a semiclassical picture, as employed in Sec. IV, the effective spin density is not quite given by the Mn impurities, but has to be reduced due to coupling to the valence-band carriers. On the other hand, x is always small since the impurity spin density N_{Mn} is larger than the itinerant-carrier concentration p and the Mn spin $S = 5/2$ is comparatively large. We, therefore, stick to the static limit in the following discussion.

IV. EASY AXIS, ENERGY GAP AND SPIN STIFFNESS

The purpose of this section is to establish the connection between the spin-wave dispersions evaluated later and the micromagnetic energy functional. The non-local magnetostatic contribution which is omitted from our theory can be added as needed in applications. The short-range part of the functional is a symmetry-adapted gradient expansion of the energy density $e[\hat{\mathbf{n}}]$. In magnetism literature the non-constant portion of the zeroth-order term $e^{\text{ani}}[\hat{\mathbf{n}}]$ is known as the magnetic anisotropy energy, and the leading gradient term $e^{\text{ex}}[\hat{\mathbf{n}}]$ is known as the exchange energy. As shown in Ref. 25 magnetic anisotropy effect in ferromagnetic semiconductors are, in the absence of strain, very well described by a cubic harmonic expansion which is truncated after sixth order,

$$e^{\text{ani}}[\hat{\mathbf{n}}] = K_1 (n_x^2 n_y^2 + n_x^2 n_z^2 + n_y^2 n_z^2) + K_2 (n_x n_y n_z)^2 \quad (18)$$

with anisotropy parameters K_1 and K_2 . Correlation of spin polarizations at different positions are described by the gradient term $e^{\text{ex}}[\hat{\mathbf{n}}]$. In order to address long-wavelength spatial fluctuations, we expand the gradient term up to lowest nonvanishing order,

$$e^{\text{ex}}[\hat{\mathbf{n}}] = \sum_{a,b \in \{x,y,z\}} A_{ab} | \partial_a n_b |^2, \quad (19)$$

with exchange parameters A_{ab} . We find in our numerical calculations that anisotropy in the exchange constant is negligibly small, i.e., we can choose $A_{ab} = A$ for all a, b , as generally assumed in the magnetism literature.

To establish the connection of the energy functional to our microscopic spin-wave calculation, we first have to determine the direction of the mean-field spin polarization and then to study small fluctuations. The first step is achieved by minimizing the energy Eq. (18). It is easy to show that the mean-field orientation $\hat{\mathbf{n}}^{\text{MF}}$ can only point along a high-symmetry axis $\langle 100 \rangle$, $\langle 110 \rangle$, $\langle 111 \rangle$, or an equivalent direction (except for the special case $K_2 = 0$ and $K_1 > 0$, where we find an easy-plane anisotropy in the planes $n_x = 0$, $n_y = 0$ or $n_z = 0$, and, of course, the isotropic case $K_1 = K_2 = 0$). In Fig. 1 we show how the mean-field polarization direction depends on K_1 and K_2 .

Now we consider small fluctuations around the mean-field orientation $\hat{\mathbf{n}}^{\text{MF}}$. The kernel of the quadratic form $e^{\text{ani}}[\hat{\mathbf{n}}] - e^{\text{ani}}[\hat{\mathbf{n}}^{\text{MF}}]$ has two eigenvalues λ_1 and λ_2 . We find for $\hat{\mathbf{n}}^{\text{MF}}$ along $\langle 100 \rangle$ that $\lambda_1 = \lambda_2 = K_1$, for $\langle 110 \rangle$ we get $\lambda_1 = -K_1$ and $\lambda_2 = (2K_1 + K_2)/4$, and for $\langle 111 \rangle$ we obtain $\lambda_1 = \lambda_2 = -(6K_1 + 2K_2)/9$. In all cases, λ_1 and λ_2 are positive. Quantizing the collective spin coordinate at long wavelengths, it follows that

$$\Omega_k = \frac{2\sqrt{\lambda_1 \lambda_2}}{N_{\text{Mn}}S} + \frac{2A}{N_{\text{Mn}}S} k^2 + \mathcal{O}(k^4). \quad (20)$$

There are two alternative ways to determine the energy gap $\Omega_{k=0}$. One can either perform the $k = 0$ limit of the spin-wave dispersion Eq. (17) or evaluate the coefficients λ_1 and λ_2 from calculating the energy for mean-field orientation $\hat{\mathbf{n}}^{\text{MF}}$ along the three high-symmetry axes $\langle 100 \rangle$, $\langle 110 \rangle$, and $\langle 111 \rangle$. The numerical effort of the latter procedure, which has been used previously in Ref. 25, is lesser for given accuracy. The virtue of the spin-wave calculation is to determine the exchange constant A .

We conclude this section with two remarks:

(i) In case that the easy axis is along $\langle 100 \rangle$ or $\langle 111 \rangle$ (as it is for all parameter sets considered in Sec. V), the energy cost of tilting the polarization axis by small angles is independent of the direction of the deflection. This is required by symmetry and indicated by the fact that λ_1 equals λ_2 . As shown in Appendix B, the term $E_{k=0}^{++}$ then vanishes, and the $k = 0$ limit of Eq. (17) is identical to the energy gap calculated from standard perturbation theory where the perturbation describes the deviation of the spin polarization from the mean-field direction.

(ii) The denominators $N_{\text{Mn}}S$ in Eq. (20) corresponds to the static limit employed in our calculation. The renormalization of the Berry's phase term due to corrections

to the static limit (see discussion in the previous section) could be accounted for by multiplying $N_{\text{Mn}}S$ with $(1-x)$.

V. NUMERICAL RESULTS FOR THE SPIN-WAVE DISPERSION

In this section we present numerical results for the spin-wave dispersion of (Ga,Mn)As. From these calculations we extract the spin stiffness as a function of the itinerant-carrier concentration p and on the exchange coupling J_{pd} . To model the sample which showed the highest transition temperature of 110K so far, we choose as parameters¹⁸ $N_{\text{Mn}} = 1 \text{ nm}^{-3}$, $p = 0.35 \text{ nm}^{-3}$, and $J_{\text{pd}} = 0.068 \text{ eV nm}^{-3}$. As a consequence, the mean-field spin-splitting gap for the itinerant carriers is $\Delta = N_{\text{Mn}}J_{\text{pd}}S = 0.17 \text{ eV}$.

A. Isotropic vs. six-band model

The origin of ferromagnetism, the nature of the spin excitations, and trends in the critical temperatures can be explained within a simple model which describes the itinerant carriers by parabolic bands.^{27–29,35} For more quantitative statements, a more realistic description of the band structure should be employed.

In Fig. 2 we show results for the isotropic model with two parabolic band with effective mass $m^* = 0.5m_e$ (a Debye cutoff k_D with $k_D^3 = 6\pi^2 N_{\text{Mn}}$ ensures that we include the correct number of magnetic ion degrees of freedom). We find for the majority-spin Fermi energy $\epsilon_F = 0.44 \text{ eV}$ measured from the bottom of the band. This yields the itinerant-carrier polarization $\xi = 0.35$. The dashed line in Fig. 2 marks the mean-field spin-flip energy, obtained by neglecting correlation. Since the spin-wave energies are far below the mean-field result, the isotropic model suggest that for these parameters correlation is very important and the critical temperature is limited by collective fluctuations. According to the classification scheme introduced in Ref. 30, the system would be in the "RKKY collective regime".

By fitting a parabola at small momenta we find $\Omega_k/\Delta = 0.0068(k/k_D)^2$ which yields $A = 0.095 \text{ meV nm}^{-1} = 0.015 \text{ pJ m}^{-1}$.

Now we use the six-band Kohn-Luttinger Hamiltonian with Luttinger parameters $\gamma_1 = 6.85$, $\gamma_2 = 2.1$, and $\gamma_3 = 2.9$ and spin-orbit coupling $\Delta_{\text{so}} = 0.34 \text{ eV}$. In the absence of the Mn ion, this model has anisotropic heavy- and light-hole bands with masses $m_h \approx 0.498m_e$ and $m_l \approx 0.086m_e$. The spirit of the naive parabolic band model is the hope that only the band with the larger density of states matters and the anisotropy is unimportant. We will see that these hopes are not fulfilled.

We find a much lower Fermi energy $\epsilon_F = 0.25 \text{ eV}$ than obtained for the isotropic model, and, therefore, a much higher itinerant-carrier spin polarization $\xi = 0.73$. By

calculating the mean-field energy for a Mn spin polarization along the three high-symmetry axes we determine the anisotropy parameters as $K_1 = 19.6 \times 10^{-6} \text{ eV nm}^{-3}$ and $K_2 = 1.6 \times 10^{-6} \text{ eV nm}^{-3}$. As a consequence, the easy axis is $\langle 100 \rangle$ and the energy gap, $\Omega_{k=0}/\Delta = 9.2 \times 10^{-5}$, is very small in comparison to the bandwidth of the spin-wave dispersion.

In Fig. 3 we show the spin-wave dispersion for wavevectors \mathbf{k} along the easy axis. We observe that the effect of $E_{\mathbf{k}}^{++}$ in Eq. (17) is negligibly small and can, therefore, be dropped. Furthermore, we find that the dispersion for a spin wave perpendicular to the easy axis cannot be distinguished from the dispersion of spin waves along the easy axis within numerical accuracy. By fitting a parabola at small momenta we find $\Omega_k/\Delta = \Omega_{k=0}/\Delta + 0.16(k/k_D)^2$ which yields $A = 2.2 \text{ meV nm}^{-1} = 0.36 \text{ pJ m}^{-1}$ (see inset of Fig. 3). Furthermore, we see that the energy gap $\Omega_{k=0}/\Delta$ determined in the previous paragraph is consistent with our spin-wave results. Employing the six-band model we see that for the given parameters the spin-wave energies are much closer to the mean-field value than for the isotropic model. According to our classification given in Ref. 30 the system is rather in the "mean-field regime", which explains the success of mean-field theory to reproduce the critical temperature.

B. Six-band model plus strain

The lattice constants of (Ga,Mn)As and GaAs do not match. Since low-temperature molecular beam epitaxy (MBE) has to be used to overcome the low solubility of Mn in GaAs, even thick films of (Ga,Mn)As grown on GaAs cannot relax to their equilibrium. The lattice of (Ga,Mn)As is instead locked to that of the underlying substrate. This induces strain which breaks the cubic symmetry. The influence of MBE growth lattice-matching strain on hole bands of cubic semiconductors is well understood.^{36,37} This effect can easily be accounted for adding a strain term to the Hamiltonian (we use Eq. (32) of Ref. 25 with strain parameters $e_0 = -0.0028$ and $\Gamma = -3.24 \text{ eV}$).

We choose the growth direction to be along $\langle 001 \rangle$ and compute the energy for five different directions $\langle 100 \rangle$, $\langle 001 \rangle$, $\langle 110 \rangle$, $\langle 011 \rangle$, and $\langle 111 \rangle$. The lowest energy is found for $\langle 100 \rangle$, i.e., we find an easy-axis anisotropy where the easy axis is in the plane perpendicular to the growth direction, in accordance with experiments.³⁸ The expansion of the mean-field anisotropy energy for small fluctuations around $\langle 100 \rangle$ is now

$$e^{\text{MF}}[\hat{\mathbf{n}}] = K_0 n_z^2 + K_1 n_x^2 n_y^2 + \tilde{K}_1 (n_x^2 n_z^2 + n_y^2 n_z^2) \quad (21)$$

with $K_0 = 20.0 \times 10^{-6} \text{ eV nm}^{-3}$, $K_1 = 19.4 \times 10^{-6} \text{ eV nm}^{-3}$, and $\tilde{K}_1 = 19.6 \times 10^{-6} \text{ eV nm}^{-3}$. The eigenvalues for small fluctuations around the $\langle 100 \rangle$ axis are $K_0 + \tilde{K}_1$ and K_1 . From this we estimate that the energy gap in the dispersion is larger than in the absence of

strain by a factor of 1.4, i.e., still small. The spin stiffness derived from the curvature of the spin-wave dispersion is identical to that in the absence of strain within the accuracy of our numerical calculations. We will, therefore, ignore the effect of strain in the following.

C. Spin stiffness

In Fig. 4 we show the exchange constant (or spin stiffness) A as a function of the itinerant-carrier density for both the isotropic two-band and the full six-band model. We find that the spin stiffness is much larger for the six-band calculation than for the two-band model. Furthermore, for the chosen range of itinerant-carrier densities the trend is different: in the two-band model the exchange constant decreases with increasing density, while for the six-band description we observe an increase with a subsequent saturation.

Experimental estimates for J_{pd} vary from 0.054 eV nm^3 to 0.15 eV nm^3 , with more recent work suggesting a value toward the lower end of this range.^{16–18} To address the dependence of the spin stiffness on J_{pd} , we show in Fig. 5 results for a J_{pd} twice as large as in Fig. 4 and find an enhancement of the exchange constant. We find that an isotropic model would also underestimate the spin stiffness considerably in this regime.

To understand this behavior we recall^{28,29} that the two-band model predicts $A = p\hbar^2/(8m^*)$ for low densities p , while at high densities A decreases as a function of p (note that in Refs. 28 and 29 the spin stiffness was characterized by $\rho = 2A$). The crossover occurs near $\Delta \sim \epsilon_F$. The difference in the trends seen for the two- and six-band model in Figs. 4,5 is consistent with the observation that, at given itinerant-carrier concentration p , the Fermi energy ϵ_F is much smaller when the six-band model is employed, where more bands are available for the carriers, than in the two-band case. Furthermore, we emphasize that, even in the limit of low carrier concentration, it is not only the (heavy-hole) mass of the lowest band which is important for the spin stiffness. Instead, a collective state in which the spins of the itinerant carriers follow the spatial variation of a Mn spin-wave configuration will involve the light-hole band, too.

CONCLUSION

In conclusion we present a microscopic calculation of micromagnetic parameters for ferromagnetic (Ga,Mn)As. We draw the connection of the anisotropy and exchange constant of a classical energy functional to the gap and curvature of the spin-wave dispersion. Numerical results for the spin stiffness as a function of itinerant-carrier concentration and $p - d$ exchange coupling are shown. We find that the energy gap is much smaller than the bandwidth, the spin stiffness is nearly isotropic, and strain

does not effect the dispersion much. Furthermore, we see that a model with isotropic valence bands underestimates the spin stiffness considerably.

ACKNOWLEDGEMENTS

We acknowledge useful discussions with M. Abolfath, B. Beschoten, T. Dietl, J. Furdyna, H.H. Lin, and J. Schliemann. This work was supported by the Deutsche Forschungsgemeinschaft, the Welch Foundation, the Indiana 21st Century Fund, and the Office of Naval Research and the Research Foundation fo the State University of New York under grant number N000140010951.

APPENDIX A: RENORMALIZATION OF BERRY'S PHASE TERM

In this section, we show that the linear correction beyond the static limit yields a correction to the Berry's phase. This accounts for the fact that the effective spin in a semiclassical approach does not have the length S of the Mn impurities by is reduced by a factor $(1 - x)$ due to coupling to the itinerant-carrier spin degree of freedom. We expand the r.h.s of Eq. (15) up to linear order in $i\nu_m$. The terms with $\bar{z}\bar{z}$ and zz vanish since it is an odd function under the following operation: we shift $\mathbf{q} \rightarrow -\mathbf{q} - \mathbf{k}$, use the fact that $\epsilon_\alpha(-\mathbf{q} - \mathbf{k}) = \epsilon_\alpha(\mathbf{q} + \mathbf{k})$ and $\epsilon_\beta(-\mathbf{q}) = \epsilon_\beta(\mathbf{q})$ and, finally, exchange $\alpha \leftrightarrow \beta$. Hence, we only have to deal with the term which involves $\bar{z}z$.

Assume that there is an operator Q such that $N_{\text{Mn}}J_{pd}Ss^+ = [H, Q]$ and $N_{\text{Mn}}J_{pd}Ss^- = -[H, Q^\dagger]$. Then the renormalization for the Berry's phase is given by $(1 - x)$ with

$$x = \frac{1}{2N_{\text{Mn}}SV} \sum_{\mathbf{q}} \sum_{\alpha} f[\epsilon_\alpha(\mathbf{q})] \langle \alpha | [Q^\dagger, Q] | \alpha \rangle \quad (\text{A1})$$

independent of \mathbf{k} . In the absence of spin-orbit coupling we choose $Q = s^+$, which yields

$$x = \frac{\langle s^z \rangle}{N_{\text{Mn}}S} = \frac{p\xi}{2N_{\text{Mn}}S}, \quad (\text{A2})$$

i.e., x is just the ratio of itinerant-carrier spin concentration to Mn spin density. For finite spin-orbit coupling the spin of the itinerant carrier is coupled to the orbital angular momentum. If the band Hamiltonian is invariant under rotation in space, we can choose $Q = s^+ + l^+$ and find

$$x = \frac{\langle s^z + l^z \rangle}{N_{\text{Mn}}S}. \quad (\text{A3})$$

In this case the correction is given by the ratio of the total angular momentum density of the itinerant carriers and the Mn concentration.

If the valence bands are described by the Kohn-Luttinger Hamiltonian, however, the total angular momentum is no longer a conserved quantity. Or, equivalently, the orbital angular momentum of the valence-band carriers couples to the crystal lattice, and the simple form Eq. (A3) no longer holds.

APPENDIX B: SPIN-WAVE DISPERSION GAP

The goal of this section is to rederive the $k = 0$ limit of the spin-wave energy Eq. (17) by standard perturbation theory where the perturbation describes the deviation of the spin polarization from the mean-field direction $\langle 100 \rangle$ or $\langle 111 \rangle$.

1. Proof that $E_{k=0}^{++} = 0$ for $\langle 100 \rangle$ or $\langle 111 \rangle$ easy axis

We start by showing that

$$E_{k=0}^{++} = -\frac{1}{V} \sum_{\mathbf{q}} \sum_{\alpha\beta} \frac{f[\epsilon_{\alpha}(\mathbf{q})] - f[\epsilon_{\beta}(\mathbf{q})]}{\epsilon_{\alpha}(\mathbf{q}) - \epsilon_{\beta}(\mathbf{q})} s_{\alpha\beta}^{+} s_{\beta\alpha}^{+} \quad (\text{B1})$$

vanishes, if the mean-field polarization is along $\langle 100 \rangle$ or $\langle 111 \rangle$. Note that α and β now label the *same* basis states.

Let $\tilde{\mathbf{q}}$ be a wavevector which is obtained from \mathbf{q} by rotation about the z -axis (which is defined by the mean-field Mn spin polarization direction) by an angle φ which respects the symmetry of the crystal. If the z -axis is $\langle 100 \rangle$ or $\langle 111 \rangle$, then the allowed angles are $\varphi \in \{0, \pi/2, \pi, 3\pi/2\}$ or $\{0, 2\pi/3, \pi, 4\pi/3\}$, respectively. For $\langle 110 \rangle$ it would be $\varphi \in \{0, \pi\}$. Due to the symmetry of the crystal, the spectrum at $\tilde{\mathbf{q}}$, labeled by $\tilde{\alpha}$ (or $\tilde{\beta}$), is identical to that at \mathbf{q} , i.e., $\epsilon_{\tilde{\alpha}} = \epsilon_{\alpha}$. The corresponding eigenstates are connected by $|\tilde{\alpha}\rangle = U|\alpha\rangle$ with $U = \exp[i(s^z + l^z)\varphi]$.

Since the spin operator s^+ and the operator for the orbital angular momentum l^z commute, the following relation is satisfied,

$$\begin{aligned} s_{\tilde{\alpha}\tilde{\beta}}^{+} s_{\tilde{\beta}\tilde{\alpha}}^{+} &= \langle \alpha | U^{-1} s^+ U | \beta \rangle \langle \beta | U^{-1} s^+ U | \alpha \rangle \\ &= e^{-2i\varphi} s_{\alpha\beta}^{+} s_{\beta\alpha}^{+}. \end{aligned} \quad (\text{B2})$$

As a consequence, the partial summation in Eq. (B1) over all wavevectors \mathbf{q} which are equivalent due to symmetry yields a factor $(1 + e^{-i\pi} + e^{-2i\pi} + e^{-3i\pi}) = 0$ for the easy axis $\langle 100 \rangle$ and $(1 + e^{-4i\pi/3} + e^{-8i\pi/3}) = 0$ for $\langle 111 \rangle$, i.e., $E_{k=0}^{++} = 0$ in both cases. In contrast, the corresponding factor $(1 + e^{-2i\pi})$ for $\langle 110 \rangle$ is nonzero, and $E_{k=0}^{++}$ is, in general, finite.

2. Relation between energy gap and $E_{k=0}^{+-}$

To determine the energy cost of tilting the spin polarization by small angle θ out of the mean-field direction, we add to the Hamiltonian the perturbation

$$H' = \Delta \left[-\frac{\theta^2}{2} s^z + \theta (s^x \cos \varphi + s^y \sin \varphi) \right], \quad (\text{B3})$$

and use standard perturbation theory. Here, $\varphi \in [0, 2\pi)$ is the azimuth, and $\Delta = N_{\text{Mn}} J_{\text{pd}} S$. The linear order in θ does not contribute since $\langle s^x \rangle = \langle s^y \rangle = 0$. To obtain the quadratic order in θ we use first-order perturbation theory for the s^z term in Eq. (B3) and second-order perturbation theory for the $s^x \cos \varphi + s^y \sin \varphi = (s^+ e^{-i\varphi} + s^- e^{i\varphi})/2$ contribution. For the former we get

$$\delta E' = -\frac{\theta^2 \Delta}{2V} \sum_{\mathbf{q}} \sum_{\alpha} f[\epsilon_{\alpha}(\mathbf{q})] \langle \alpha | s^z | \alpha \rangle = \frac{\theta^2 \Delta p \xi}{4}, \quad (\text{B4})$$

and the result for latter reads

$$\begin{aligned} \delta E'' &= \frac{\theta^2 \Delta^2}{4V} \sum_{\mathbf{q}} \sum_{\alpha\beta} f[\epsilon_{\alpha}(\mathbf{q})] \frac{|\langle \alpha | s^+ e^{-i\varphi} + s^- e^{i\varphi} | \beta \rangle|^2}{\epsilon_{\alpha}(\mathbf{q}) - \epsilon_{\beta}(\mathbf{q})} \\ &= -\frac{\theta^2 \Delta^2}{8} (2E_{k=0}^{+-} + e^{-2i\varphi} E_{k=0}^{++} + e^{2i\varphi} E_{k=0}^{--}). \end{aligned} \quad (\text{B5})$$

If the easy axis is along $\langle 100 \rangle$ or $\langle 111 \rangle$, then $E_{k=0}^{++} = E_{k=0}^{--} = 0$, and the energy is independent of φ . The spin wave energy at $k = 0$ can now be obtained from the ratio of the energy change $\delta E' + \delta E''$ and the change of the spin $\delta S = \theta^2 N_{\text{Mn}} S/2$, which yields

$$\frac{\Omega_{k=0}}{\Delta} = \frac{J_{\text{pd}}}{2} \left(\frac{p \xi}{\Delta} - E_{k=0}^{+-} \right), \quad (\text{B6})$$

and, as desired, we recover the $k = 0$ limit of Eq. (17) for an easy-axis direction $\langle 100 \rangle$ or $\langle 111 \rangle$.

¹ G.A. Prinz, Physics Today **48**, April issue, 58 (1995).

² G.A. Prinz, Science **282**, 1660 (1998).

³ J.K. Furdyna and J. Kossut, *Diluted Magnetic Semiconductors*, Vol. 25 of *Semiconductor and Semimetals* (Academic Press, New York, 1988).

⁴ T. Dietl, *Diluted Magnetic Semiconductors*, Vol. 3B of *Handbook of Semiconductors*, (North-Holland, New York, 1994).

⁵ A. Haury, A. Wasiela, A. Arnoult, J. Cibert, S. Tatarenko, T. Dietl, Y. Merle d' Aubigné, Phys. Rev. Lett. **79**, 511 (1997).

⁶ H. Ohno, H. Munekata, T. Penney, S. von Molnár, and L.L. Chang, Phys. Rev. Lett. **68**, 2664 (1992).

⁷ H. Ohno, A. Shen, F. Matsukura, A. Oiwa, A. Endo, S. Katsumoto, and Y. Iye, Appl. Phys. Lett. **69**, 363 (1996).

⁸ H. Ohno, Science **281**, 951 (1998).

⁹ H. Ohno, J. Magn. Magn. Mater. **200**, 110 (1999).

¹⁰ T. Hayashi, M. Tanaka, K. Seto, T. Nishinaga, H. Shimada, and K. Ando, J. Appl. Phys. **83**, 6551 (1998).

¹¹ T.M. Pekarek, B.C. Crooker, I. Miotkowski, and A.K. Ramdas, J. Appl. Phys. **83**, 6557 (1998).

¹² A. Van Esch, J. De Boeck, L. Van Bockstal, R. Bogaerts, F. Herlach, and G. Borghs, *J. Phys. Condensed Matter* **9**, L361 (1997).

¹³ A. Van Esch, L. Van Bockstal, J. De Boeck, G. Verbanck, A.S. van Steenbergen, P.J. Wellmann, B. Grietens, R. Bogaerts, F. Herlach, and G. Borghs, *Phys. Rev. B* **56**, 13103 (1997).

¹⁴ A. Oiwa, A. Endo, S. Katsumoto, Y. Iye, H. Ohno, and H. Munekata, *Phys. Rev. B* **59**, 5826 (1999).

¹⁵ F. Matsukura, H. Ohno, A. Shen, and Y. Sugawara, *Phys. Rev. B* **57**, R2037 (1998).

¹⁶ H. Ohno, N. Akiba, F. Matsukura, A. Shen, K. Ohtani, and Y. Ohno, *Appl. Phys. Lett.* **73**, 363.

¹⁷ J. Okabayashi, A. Kimura, O. Rader, T. Mizokawa, A. Fujimori, T. Hayashi, and M. Tanaka, *Phys. Rev. B* **58**, R4211 (1998).

¹⁸ T. Omiya, F. Matsukura, T. Dietl, Y. Ohno, T. Sakon, M. Motokawa, and H. Ohno, *Physica E* **7**, 976 (2000).

¹⁹ B. Beschoten, P.A. Crowell, I. Malajovich, D.D. Awschalom, F. Matsukura, A. Shen, and H. Ohno, *Phys. Rev. Lett.* **83**, 3073 (1999).

²⁰ R. Skomski and J.M.D. Coey, *Permanent Magnetism* (Institute of Physics Publishing, Bristol, 1999).

²¹ T. Dietl, A. Haury, and Y.M. d'Aubigné, *Phys. Rev. B* **55**, R3347 (1997).

²² T. Jungwirth, W.A. Atkinson, B.H. Lee, and A.H. MacDonald, *Phys. Rev. B* **59**, 9818 (1999).

²³ T. Dietl, H. Ohno, F. Matsukura, J. Cibert, and D. Ferrand, *Science* **287**, 1019 (2000).

²⁴ B.H. Lee, T. Jungwirth, and A.H. MacDonald, *Phys. Rev. B* **61**, 15606 (2000).

²⁵ M. Abolfath, T. Jungwirth, J. Brum, and A.H. MacDonald, *Phys. Rev. B* **63**, 054418 (2001).

²⁶ T. Dietl, H. Ohno, and F. Matsukura, cond-mat/0007190.

²⁷ J. König, H.H. Lin, and A.H. MacDonald, *Phys. Rev. Lett.* **84**, 5628 (2000).

²⁸ J. König, H.H. Lin, and A.H. MacDonald, to be published in *Physica E* (2001).

²⁹ J. König, H.H. Lin, and A.H. MacDonald, cond-mat/0010471, to be published in *Interacting Electrons in Nanostructures*, edited by R. Haug and H. Schoeller (Springer).

³⁰ J. Schliemann, J. König, H.H. Lin, and A.H. MacDonald, cond-mat/0010036; accepted for publication in *Appl. Phys. Lett.*

³¹ J. Schliemann, J. König, and A.H. MacDonald, cond-mat/0012233, submitted to *Phys. Rev. B*.

³² J.M. Luttinger and W. Kohn, *Phys. Rev.* **97**, 869 (1955).

³³ S. Sanvito, P. Ordejón, and N.A. Hill, cond-mat/0011050.

³⁴ A. Auerbach, *Interacting Electrons and Quantum Magnetism* (Springer, New York, 1994).

³⁵ P. Lyu and K. Moon, cond-mat/0101206.

³⁶ W.W. Chow and S.W. Koch, *Semiconductor-Laser Fundamentals* (Springer, Berlin, 1999).

³⁷ G.L. Bir and G.E. Pikus, *Symmetry and Strain-Induced Effects in Semiconductors* (Wiley, New York, 1974).

³⁸ H. Ohno, F. Matsukura, A. Shen, Y. Sugawara, A. Oiwa, A. Endo, S. Katsumoto, and Y. Iye, in *Proceedings of the 23rd International Conference on the Physics of Semiconductors* (World Scientific, Singapore, 1996).

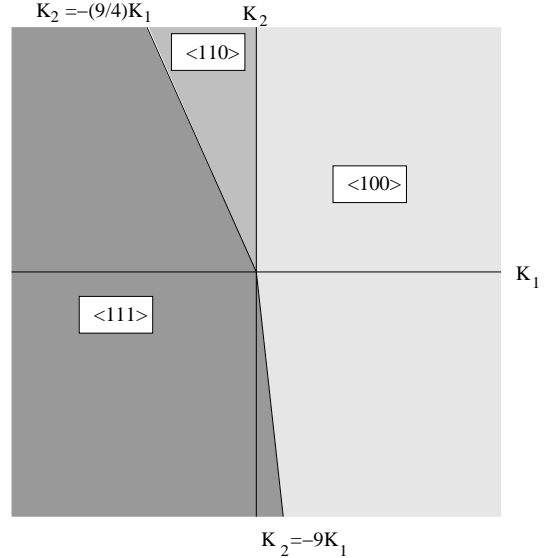


FIG. 1. Easy-axis direction as a function of K_1 and K_2 .

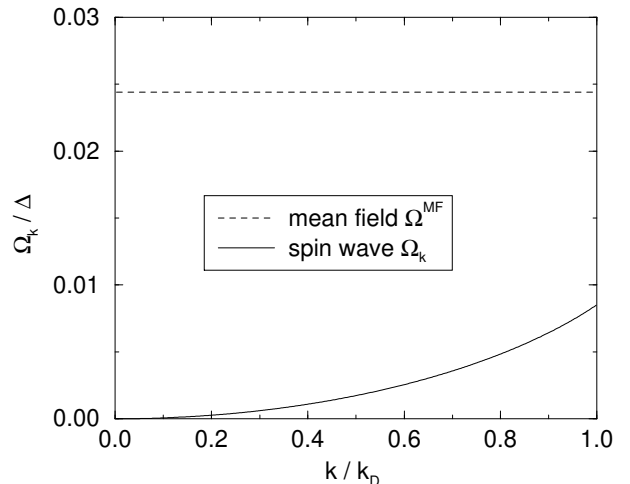


FIG. 2. Spin-wave dispersion for the isotropic model for itinerant-carrier density $p = 0.35 \text{ nm}^{-3}$, impurity-spin concentration $N_{\text{Mn}} = 1.0 \text{ nm}^{-3}$ and exchange coupling $J_{\text{pd}} = 0.068 \text{ eV nm}^{-3}$ (which yields $\Delta = 0.17 \text{ eV}$).

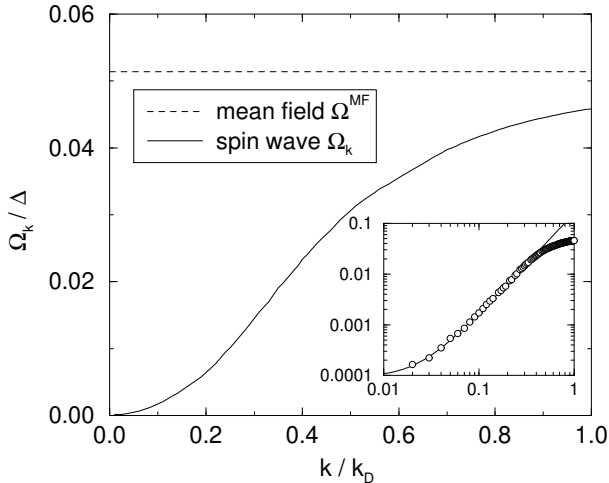


FIG. 3. Main panel: Spin-wave dispersion for the 6-band model for itinerant-carrier density $p = 0.35 \text{ nm}^{-3}$, impurity-spin concentration $N_{\text{Mn}} = 1.0 \text{ nm}^{-3}$ and exchange coupling $J_{\text{pd}} = 0.068 \text{ eV nm}^{-3}$ (which yields $\Delta = 0.17 \text{ eV}$). The momentum k is chosen to be parallel to the easy axis $\langle 100 \rangle$. Inset: Spin-wave dispersion on a log-log plot (circles) and the fit $9.2 \times 10^{-5} + 0.16(k/k_D)^2$ (solid line).

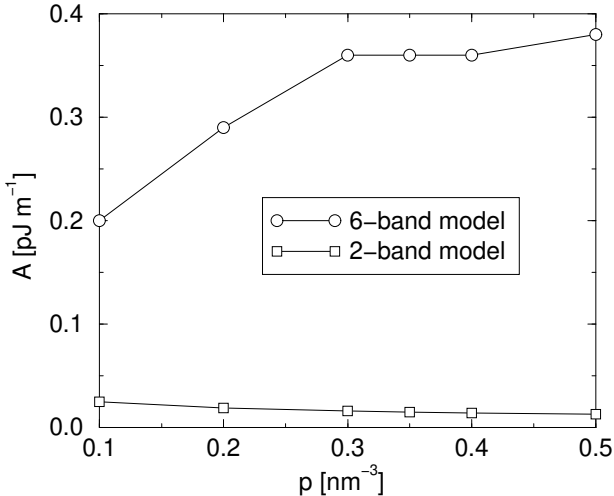


FIG. 4. Exchange constant A as a function of itinerant-carrier density p for the six-band and the two-band model. The impurity-spin concentration and the exchange coupling are chosen as $N_{\text{Mn}} = 1.0 \text{ nm}^{-3}$ and $J_{\text{pd}} = 0.068 \text{ eV nm}^{-3}$, respectively, which yields $\Delta = 0.17 \text{ eV}$.

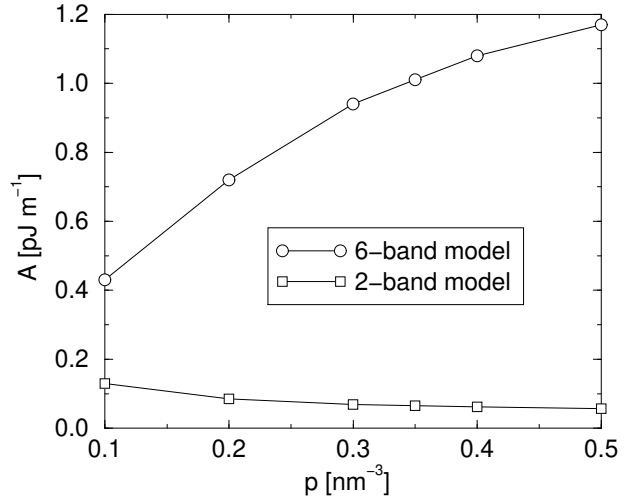


FIG. 5. Exchange constant A as a function of itinerant-carrier density p for the six-band and the two-band model. The impurity-spin concentration is chosen $N_{\text{Mn}} = 1.0 \text{ nm}^{-3}$ as in Fig. 4, but the exchange coupling $J_{\text{pd}} = 0.136 \text{ eV nm}^{-3}$ is twice as large as in Fig. 4, i.e., here we have $\Delta = 0.34 \text{ eV}$.